C201 Viscous Flow and Turbulence

Lecture 1

Part 2: Correlations

Luca di Mare

St John’s College

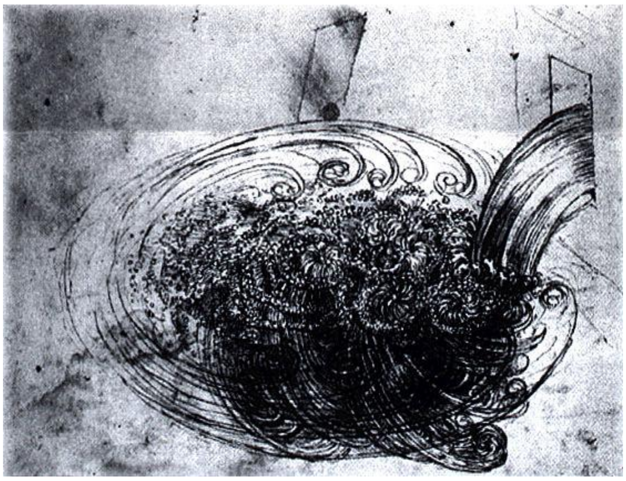

Figure 1: Leonardo’s sketch of flowing water (ca AD 1500).

1 The length and time scales of turbulent flows

In the previous section we derived formal relations that determine the mean behaviour of a turbulent flow as well as budget equations for the kinetic energy of the mean flow and – crucially – turbulence.

We have not addressed the observations made at the beginning of this module that turbulent flow fields are highly three dimensional and exhibit very complex flow patterns.

The the complex flow patterns of turbulent flow even attracted the attention of Leonardo da Vinci (14(?)April 1452– 2 May 1519). Leonardo was a keen observer of natural phenomena and noted that in a river:

"The small eddies are almost numberless, and large things are rotated only by large eddies and not by small ones, and small things are turned by both small eddies and large".

Leonardo drew a sketch, reproduced in Figure 1, to complement his notes. Even though he didn’t have mathematical tools to formulate a quantitative theory of turbulence, Leonardo had realised that turbulent flows contain flow structures – eddies – of sizes distributed over a broad range. The idea that the energy of turbulence is distributed over a continuum spectrum is cardinal in modern theories about turbulence and can be summed up by Richardson's (Lewis Fry Richardson FRS, 11 October 1881 – 30 September 1953) limerick:

"Big whirls have little whirls that feed on their velocity, and little whirls have lesser whirls and so on to viscosity."

From his Weather Prediction by Numerical Process, published in 1922.

2 Correlations between flow variables

In the previous section we have encountered the product between two fluctuating components, and we have seen that it is not, in general, zero. We can now explore how such a product could be formed and what it can tell us about a turbulent flow.

We can start by performing an experiment consisting in taking simultaneous measurements from two probes immersed in the turbulent flow at different positions, as shown in Figure 2.

The outcomes of the two measurements will be two signals, v_1 and v_2. A typical example of the variation in time of v_1 and v_2 is shown in Figure 3. The chaotic nature of turbulent flows guarantees that, as long as the probes are placed at a finite distance from each other, their outputs will be different. In Figure 3 we can however identify a vague resemblance between the two signals. This vague resemblance is quantified by the correlation $\overline{v_1' v_2'}$. If the two probes are measuring the same quantity, e.g. the x-velocity component, then we talk about auto-correlation.

2.1 Two-point correlations

In the situation considered in the previous section, the correlation $\overline{v_1' v_2'}$ compares the output of two probes placed at different positions and is therefore called a *two-point* correlation.

$$\overline{v_1' v_2'} = \lim_{T \to \infty} \frac{1}{T} \int_{\tau}^{\tau + T} v'(t, x) v'(t, x + \Delta x) dt$$

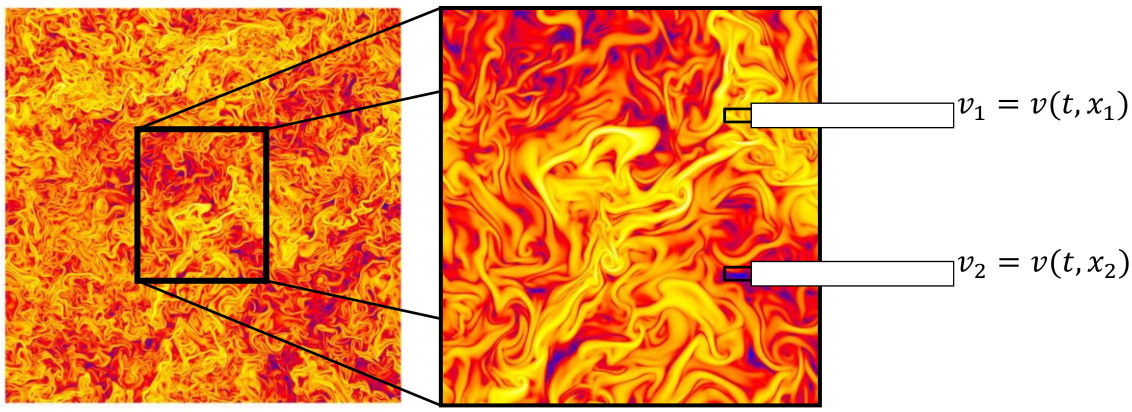

Figure 2: two probes immersed in a turbulent flow field taking simultaneous measurements v_1 and v_2.

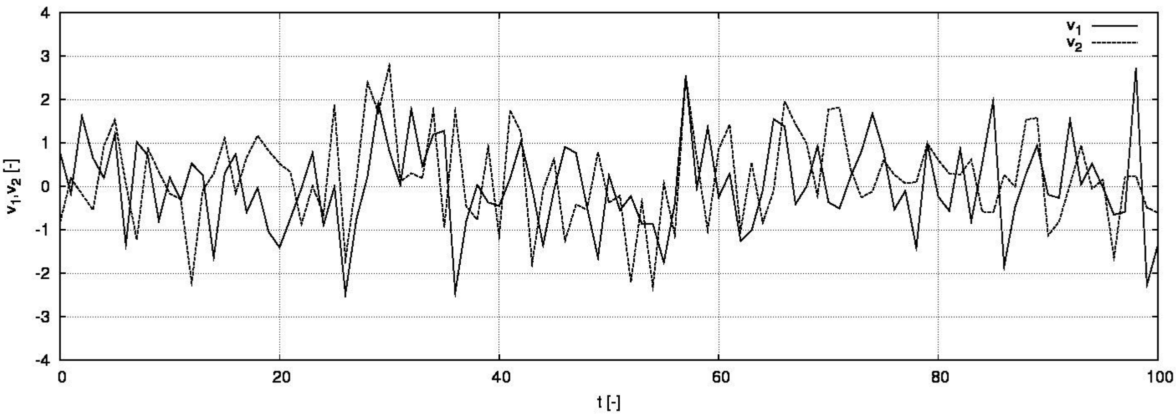

Figure 3: typical variation in time of the signals v_1 and v_2 produced by two probes immersed in a turbulent flow field.

The typical variation of a two-point correlation is shown in Figure 4. The two-point correlation is a function of the separation vector Δx. Two-point correlations typically reach a maximum value at 0 separation and decays to 0 for large separations.

The reason for this behaviour is the finite size of flow structures – usually called eddies – making up the fluctuating part of a turbulent flow. When the two probes producing the signals v_1 and v_2 are placed close to each other, their outputs are very similar because they are immersed in the same flow structure. This results in a large correlation between their outputs at small separations. When the probes are placed at a large distance from each other they are immersed in different flow structures, that evolve largely independently of each other and therefore the outputs from the two probes are uncorrelated.

The decay of two-point correlations at large separations is a consequence of the finite size of the flow structures encountered in turbulent flows.

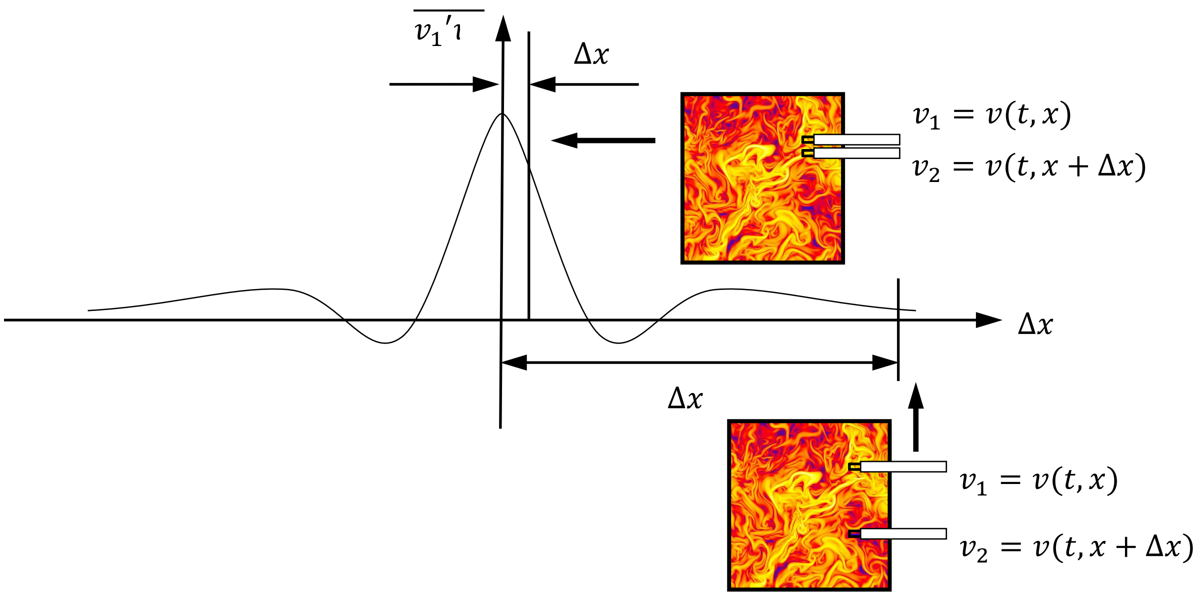

Figure 4: typical variation of a two-point correlation

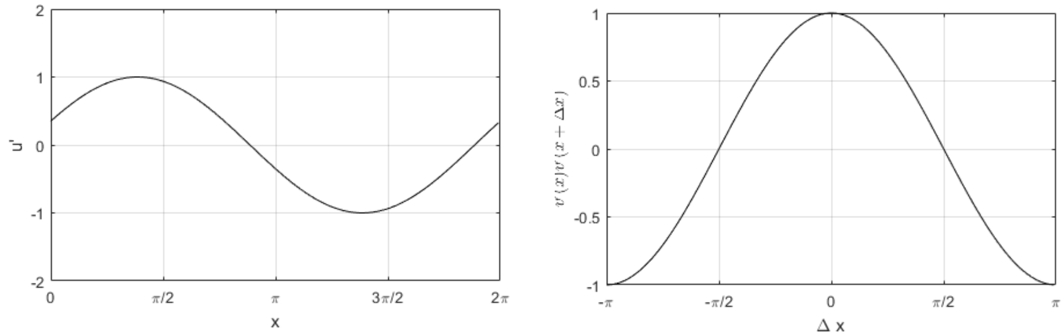

Figure 5: a random variable containing a single harmonic has the cosine function as two-point correlation.

2.1.1 Two point correlations and shape of the signal

We would like to investigate the relation between the appearance of the signal and the shape of the two-point correlation it generates.

In order to do so we construct a very simple "flow" field, made of a single variable in a one-dimensional domain. The domain is the interval $[0{:}\,2\pi]$ and the variable is constructed as the superposition of a certain number of harmonic functions, each with fixed amplitude but with random phase θ_k.

$$u' = \sum E(k)\, e^{ikx+\theta_k}$$

If u' only contains one harmonic, each realization of the flow is a single cosine function with argument shifted by a random amount. It is easy to verify that such a random variable generates a two-point correlation that is itself a cosine function with the same wave-length (see Figure 5).

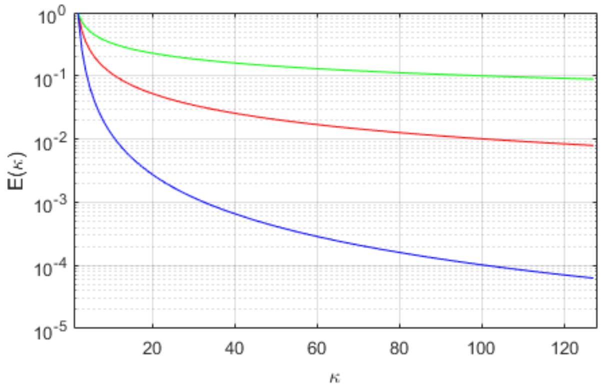

Figure 6 The function $E(k)$ for $\beta = -2, -1, -1/2$ (respectively blue,red and green curves)

.We now want to see what happens if we consider more general functions $E(k)$. We try functions of the type

$$E(k) = \alpha\, k^{\beta}$$

The graphs of the function $E(k)$ for $\beta = -2, -1, -1/2$ are shown in Figure 6.

Typical realizations of the flow and the corresponding two-point correlations are shown in Figure 7 to Figure 9. When $\beta = -2$ the function $E(k)$ decays rapidly and the contribution of high wave-numbers to the signal is small. The signal is still recognisable as an essential pure harmonic and its correlation differs very little from the shape of the cosine function.

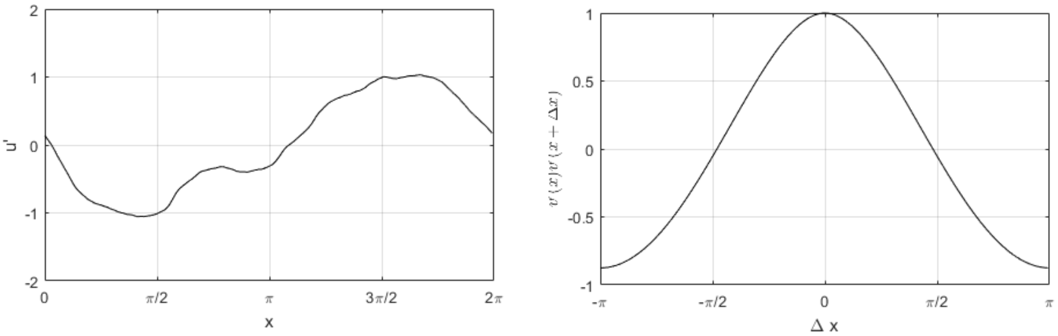

Figure 7: typical flow realization and two-point correlation for $\beta = -2$.

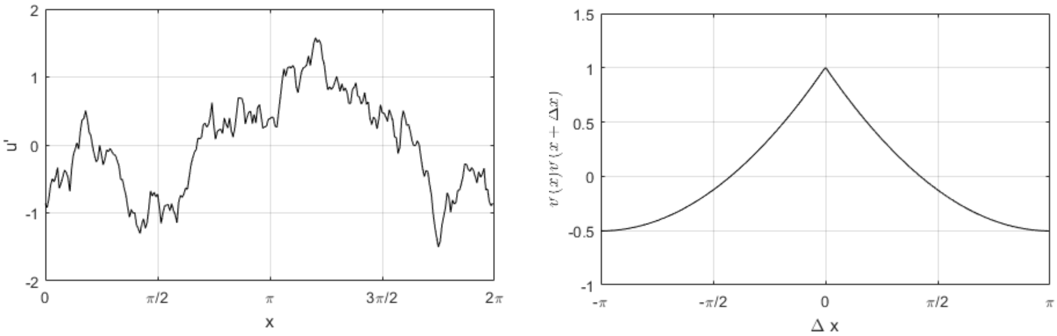

Figure 8: typical flow realization and two-point correlation for $\beta = -1$.

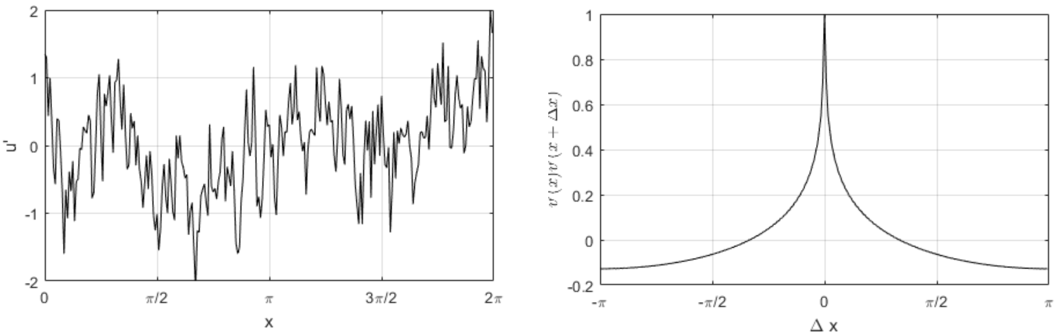

Figure 9: typical flow realization and two-point correlation for $\beta = -1/2$.

When $\beta = -1$ the contributions of high wave-numbers to the signal is clearly identifiable. The change of the correlation changes significantly and now it develops a sharp peak at 0 separation. The two-point correlation responds to the presence of small structures in the flow by decaying quicker away from its 0-separation maximum.

Finally, when $\beta = -1/2$ the contribution of small scales ot the signal is comparatively quite large and the signal starts looking like white noise. The correlation becomes even sharper and decays even quicker away from zero separation.

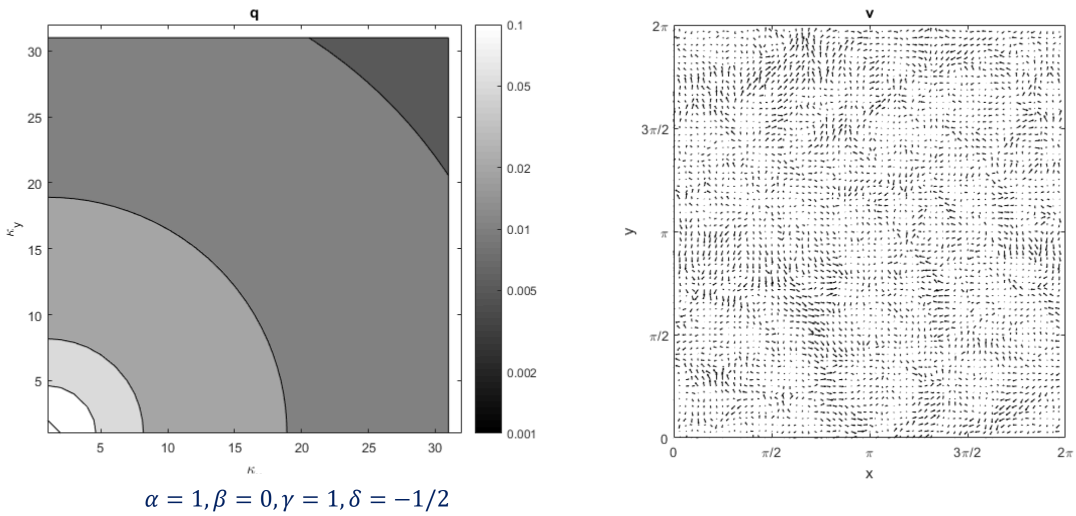

Figure 10: the function $E(\kappa_x, \kappa_y)$ for $\delta = -1$ (left) and a quiver plot of a typical realization of the flow field

2.1.2 Two-point correaltions with velocities

If the variable we are studying is a vector, then the correlation is a tensor:

$$\sigma_{ij}(x, \Delta x) = \lim_{T \to \infty} \frac{1}{T} \int_{\tau}^{\tau+T} u_i'(t, x) u_j'(t, x + \Delta x) dt$$

We would like to study the relation between the smoothness of the vector field and the shape if its correlation tensor.

We can construct a simple velocity field of the type:

$$\begin{bmatrix} u' \\ v' \end{bmatrix} = \begin{bmatrix} \hat{u} \\ \hat{v} \end{bmatrix} e^{i(\kappa_x x + \kappa_y y + \theta_\kappa)}$$

θ_κ is a random phase, just like in the previous section.

We notice that $\hat{u}$ and $\hat{v}$ are not independent because of continuity:

$$\frac{\partial u}{\partial x} + \frac{\partial v}{\partial y} = 0 \to i\kappa_x \hat{u} + i\kappa_y \hat{v} = 0$$

So we need to limit ourselves to velocity vectors in Fourier space orthogonal to the wave-numbervector:

$$\begin{bmatrix} \hat{u} \\ \hat{v} \end{bmatrix} = \frac{E(\kappa_x, \kappa_y)}{\sqrt{\kappa_x^2 + \kappa_y^2}} \begin{bmatrix} \kappa_y \\ -\kappa_x \end{bmatrix}$$

We only have the function $E(\kappa_x, \kappa_y)$ left to construct. We can choose a bilinear form:

$$E(\kappa_x, \kappa_y) = \left(\begin{bmatrix} \kappa_x \\ \kappa_y \end{bmatrix}^{\intercal} \begin{bmatrix} \alpha & \beta \\ \beta & \gamma \end{bmatrix} \begin{bmatrix} \kappa_x \\ \kappa_y \end{bmatrix} \right)^{\delta}$$

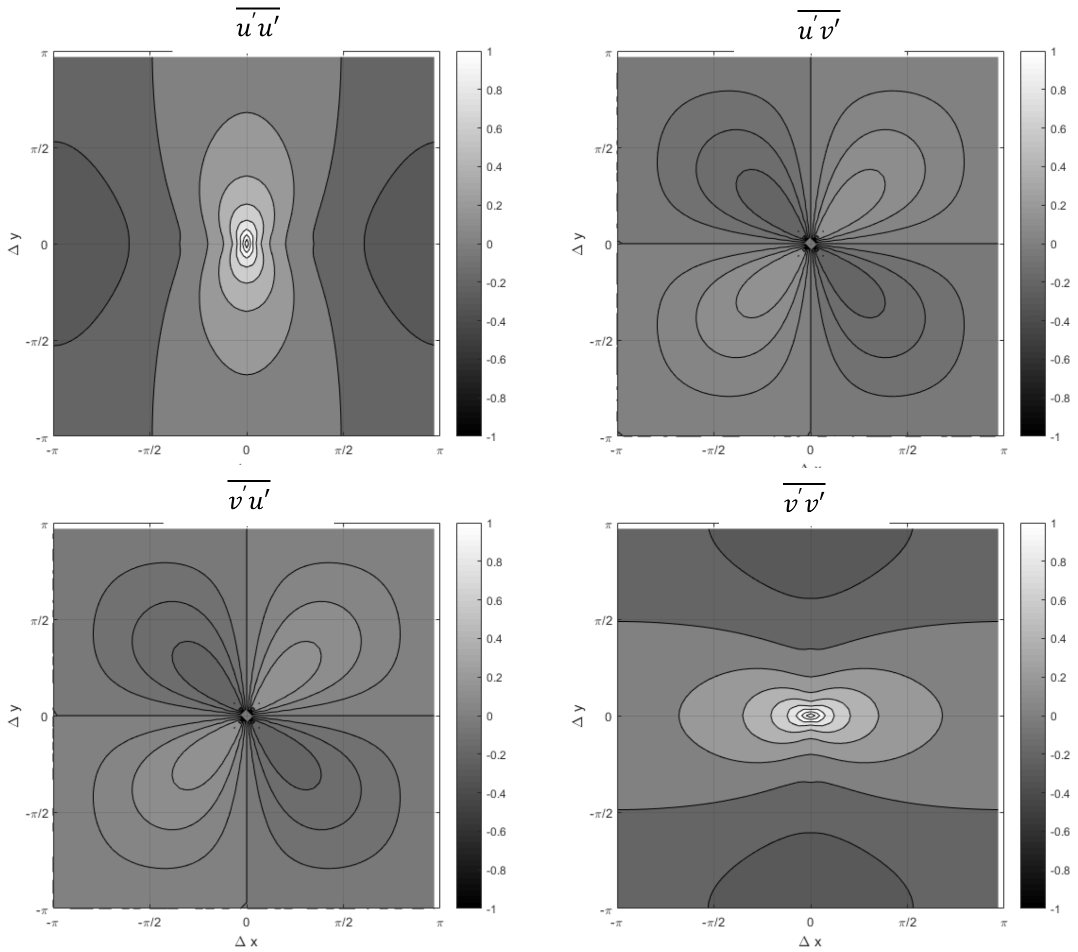

Figure 11: components of the two-point correlation tensor for the flow in Figure 10

Contours of the function $E(\kappa_x, \kappa_y)$ and a quiver plot with a typical realization of the vector field are shown in Figure 10 and the corresponding components of the correlation tensor are shown in Figure 11.

We could now modify the function $E(\kappa_x, \kappa_y)$.As an example, we could increase the magnitude of the exponent δ, so that the function $E(\kappa_x, \kappa_y)$ decays faster for large wavenumbers and the vector field is smoother. The corresponding $E(\kappa_x, \kappa_y)$ a realization of the vector field and the corresponding correlations are shown in Figure 12 and Figure 13.

Once again we notice that the smoother the vector field, the smoother the correlation tensor and the slower it decays away from the 0-separation value.

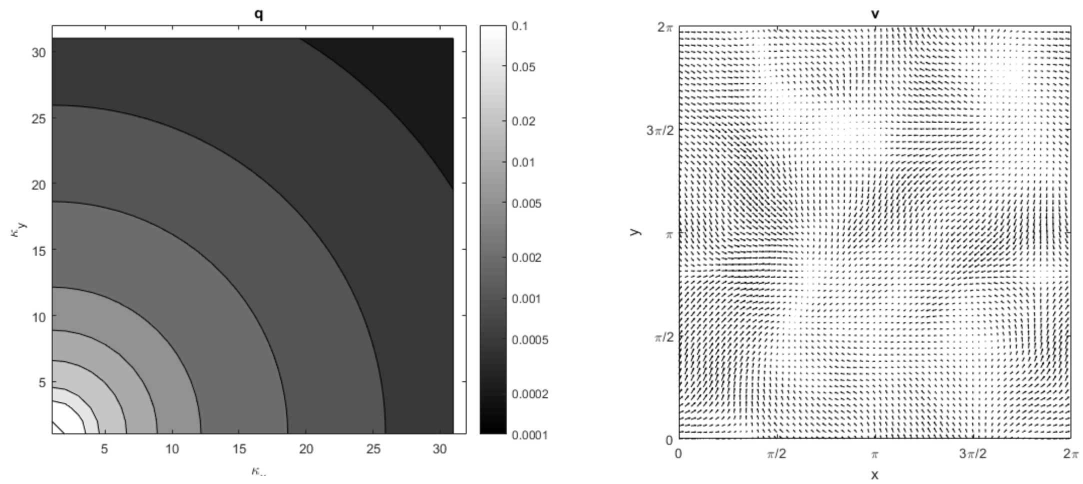

$\alpha = 1, \beta = 0, \gamma = 1, \delta = -1$

Figure 12: a smoother flow field

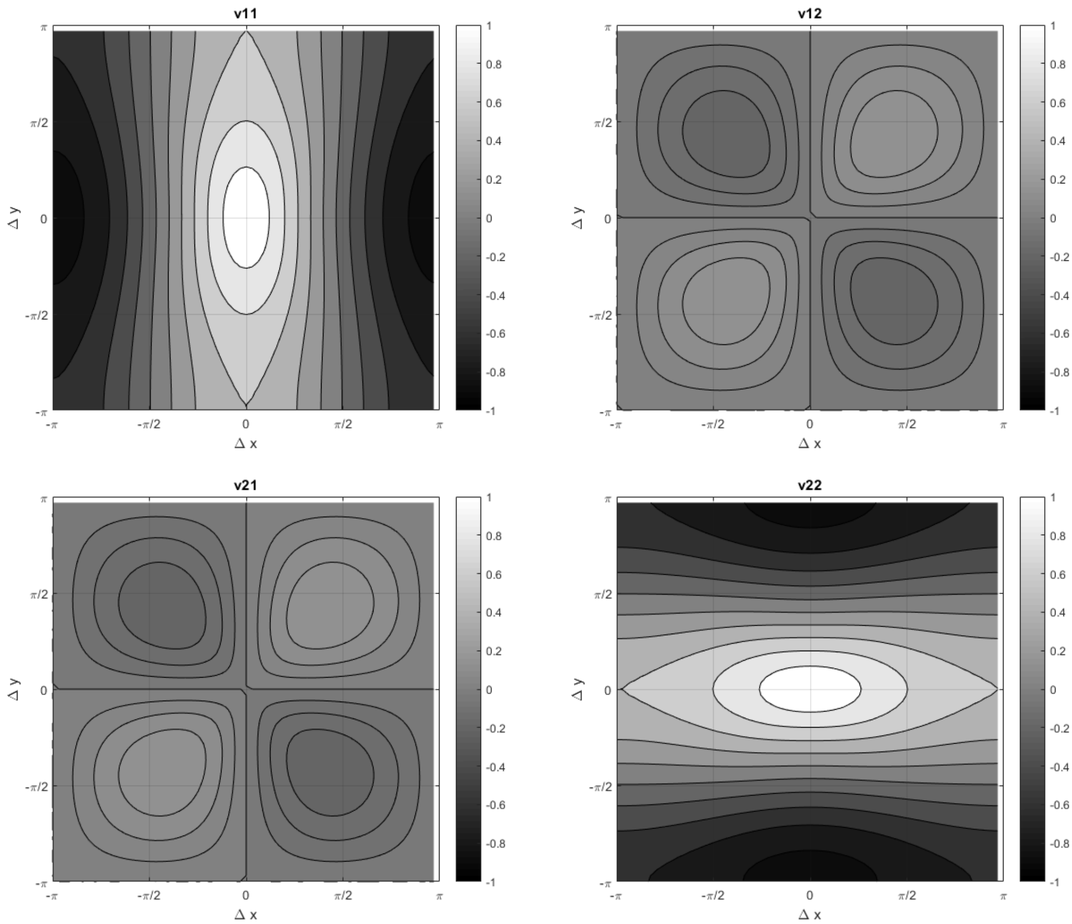

Figure 13: and its two-point correlation tensor.

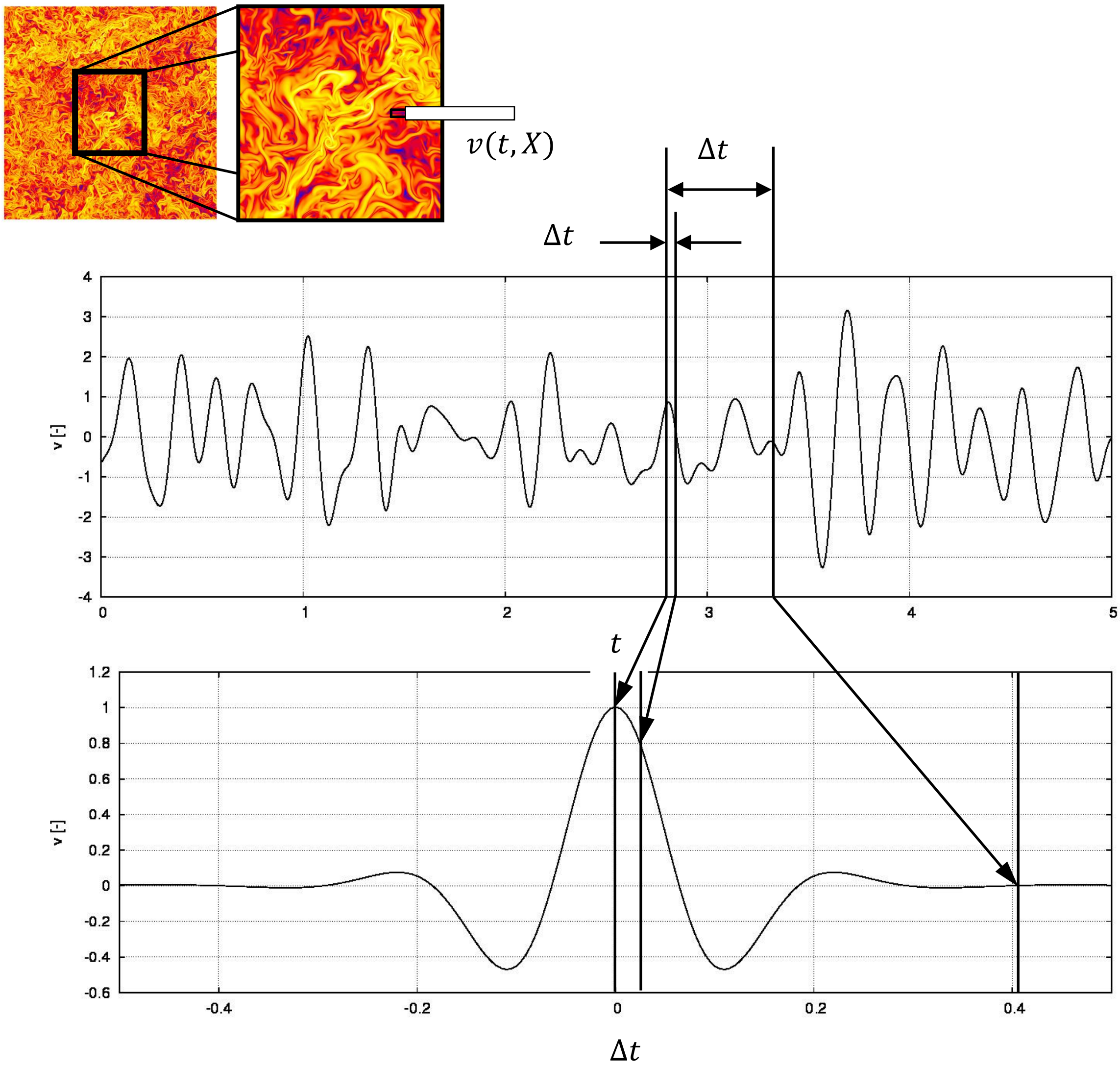

Figure 14: two-time correlation.

2.2 Correlations with time separation

We define two-point correlations by comparing the output of two probes placed simultaneously at two position in the flow field. We can similarly define two-time correlations by comparing the output of a single probe at a given time t with the output of the same probe at a later time $t + \Delta t$.

$$\overline{v'(t)v'(t+\Delta t)} = \lim_{T\to\infty} \frac{1}{T} \int_{\tau}^{\tau+T} v'(t,X)v'(t+\Delta t, X)dt$$

For a statistically stationary flow, the resulting correlation is a function of the time separation and position only. The position variable X in the definition above is historically intended as a Lagrangean variable: the probe taking the measurements is travelling at the velocity of the mean flow.

The typical variation of a two-time correlation is shown in Figure 14. At small time separations the outputs from the probe are well correlated because the probe is immersed in the same flow structure. At large time separations, the outputs from the probe become poorly correlated because the flow structure initially seen by the probe has been destroyed and has mixed with its surroundings. Its place has been taken by new structures, their histories independent of the distant past.

The decay of time correlations at large time separation is an indication of the finite lifespan of flow structures.

The small value of the two-time correlation coefficient at large time separations gives a quantitative statement to the property of unpredictability we first stated at the beginning of this module.

2.3 The integral scale

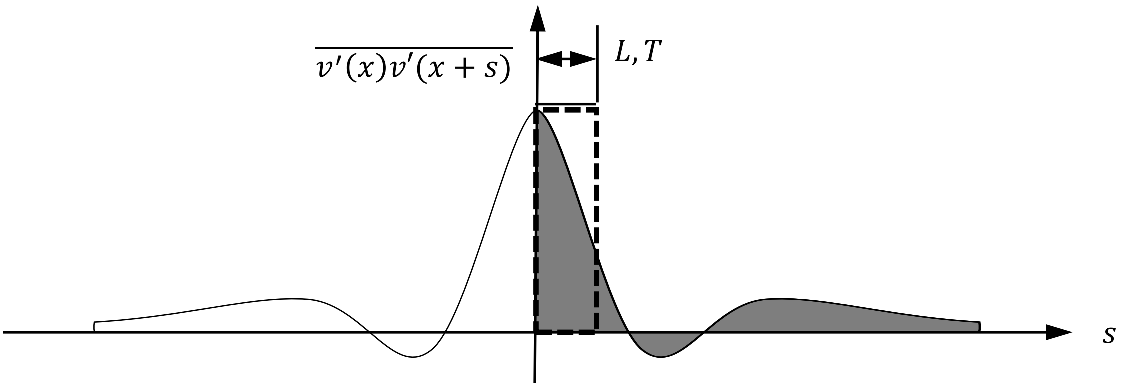

Figure 15: the integral length and time scales from an idealised version of a correlation function

We have seen that the way two-point and two-time correlations decay at large space or time separations is related to the size and lifespan of flow structures. This observation suggests that we could extract estimates for these quantities – size and lifespan of turbulent eddies – from the graphs of two-point and two-time correlations.

The idea is to reduce the measured smooth variation of the correlation function to a discontinuous function that has value 1 up to a suitably chosen separation L and takes the value 0 after that. We can identify the separation L as the distance beyond which no significant correlation is found in two-points statistics and therefore L is an indication of the size of the largest structures in the flow. If our idealised correlation function is to have the same integral as the measured correlation function, then

$$L = \frac{1}{\overline{v'(t,x)v'(t,x)}} \int_0^\infty \overline{v'(t,x)v'(t,x+s)}ds$$

The quantity L thus defined is the integral length scale.

We can similarly define an integral time scale T which represents the lifespan of the largest structures in the flow

$$T = \frac{1}{\overline{v'(t,x)v'(t,x)}} \int_0^\infty \overline{v'(t,x)v'(t+s,x)}ds$$

Integral scales are typically related to the geometry of the flow. As an example, the integral scale in turbulent flow in a pipe is the diameter of the pipe. The integral scale in turbulent flow past an obstacle is the obstacle size.

In general, we believe that integral scales (both length and time) are finite on physical grounds and many results in the theory of turbulence are based on this hypothesis.

2.4 The Taylor microscale

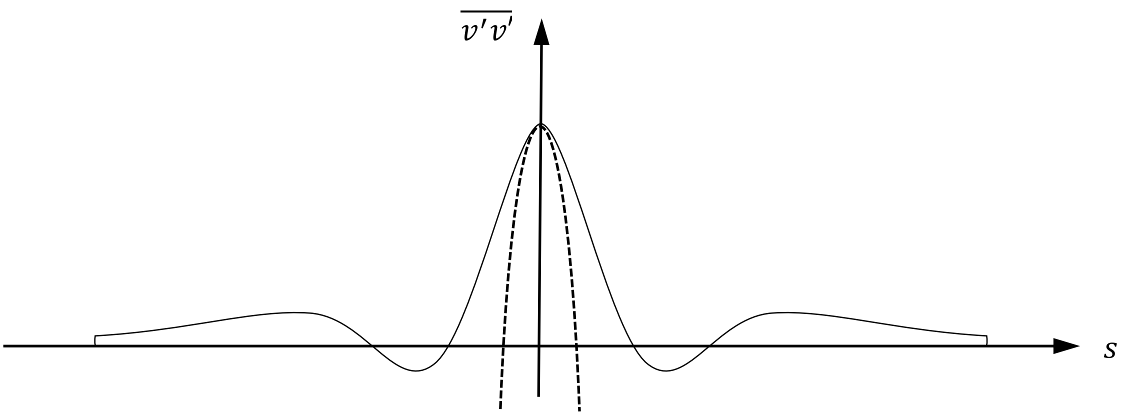

Figure 16: the Taylor microscale

The area under the correlation function graph gives us a measure of the largest time- or length-scales in the flow. We can also obtain information about the smallest scales if we analyse the graph of the auto-correlation at zero separations.

The general idea is that auto-correlations must have a maximum at zero separation because zero separation represents the condition when two probes are producing identical output, or a comparison of the signal with itself if we are looking at two-time statistics.

The rate at which the auto-correlation of a turbulent variable decays away from zero separation is dictated by its second derivative. Physically, the auto-correlation starts decaying at small separations because of small scale fluctuations. Indeed, these fluctuations are the smallest (in terms of length- or time-scale) detectable in the flow.

The scale of these fluctuations is given by the second derivative of the auto-correlations and it is called the Taylor microscale, after G.I. Taylor.

More precisely, the Taylor microscale λ in space is given by

$$-\frac{2}{\lambda^2} = \frac{1}{\overline{v'(t,x)v'(t,x)}} \frac{\partial^2}{\partial^2 s} \overline{v'(t,x)v'(t,x+s)}$$

and in time:

$$-\frac{2}{\tau^2} = \frac{1}{\overline{v'(t,x\,)v'(t,x)}} \frac{\partial^2}{\partial^2 s} \overline{v'(t+s,x)v'(t,x)}$$

The Taylor microscale indicates the limit beyond which viscosity no longer affects the flow. It can be shown that

$$\frac{\overline{u'^2}}{\lambda^2} \propto \overline{\left(\frac{\partial v'}{\partial x}\right)^2}$$

2.5 The energy spectrum

We now set off to establish relations between the way energy is distributed across length- or time-scales in a turbulent flow, the properties of the autocorrelation function and the Fourier transforms of the flow quantities.

We start by writing the Fourier integral for a fluctuating flow quantity $u'(t)$. $u'(t)$ could be a velocity component measured by a probe immersed at a fixed location in the flow:

$$u'(t) = \int \hat{u}(\kappa) e^{i\kappa t}\, d\kappa$$

By writing the Fourier integral for $u'(t)$ we are stating that $u'(t)$ contains harmonically varying components with frequencies κ and amplitude $\hat{u}(\kappa)$.

Consider now the auto-correlation $\sigma(s)$

$$\sigma(s) = \overline{u'(t)u'^*(t+s)}$$

$$\sigma(s) = \lim_{T\to\infty} \frac{1}{T} \int_0^T u'(t)u'^*(t+s)dt$$

$\sigma(s)$ has all the properties of the correlation functions discussed earlier. In view of the Fourier integral for $u'(t)$ we can write

$$\sigma(s) = \lim_{T\to\infty} \frac{1}{T} \int_0^T \left(\int \hat{u}(\kappa) e^{i\kappa t}\, d\kappa\right)\left(\int \hat{u}^*(\kappa') e^{-i\kappa'(t+s)}\, d\kappa'\right) dt$$

The integrals over κ and κ' are independent of each other and their order can be swapped:

$$\sigma(s) = \int \int \hat{u}(\kappa)\hat{u}^*(\kappa') \left(\lim_{T\to\infty} \frac{1}{T} \int_0^T e^{i(\kappa-\kappa')t} dt\right) e^{-i\kappa' s}\, d\kappa\, d\kappa'$$

We now need to give some thought to the term in brackets:

$$\lim_{T\to\infty} \frac{1}{T} \int_0^T e^{i(\kappa-\kappa')t} dt$$

If $\kappa = \kappa'$, then the integral is T and the term has value 1.

If $\kappa \neq \kappa'$ then the integral is indefinite, but it has a finite value because $e^{i\theta} = cos\theta + i\sin\theta$. When taking the limit for $T \to \infty$, the factor $1/T \to 0$ so the whole limit tends to 0. We are therefore left with:

$$\sigma(s) = \int \hat{u}(\kappa)\hat{u}^*(\kappa)e^{-i\kappa s}\,d\kappa$$

We are therefore left with the important result that the Fourier transform of the correlation $\sigma(s)$ is directly related to the Fourier transform of the signal $u'(t)$

$$\sigma(s) = \int \hat{u}(\kappa)\hat{u}^*(\kappa)e^{-i\kappa s}\,d\kappa$$

Furthermore,

$$\sigma(s) = \int |\hat{u}(\kappa)|^2\, e^{-i\kappa s}\,d\kappa$$

$$\sigma(s) = \int E(\kappa)\, e^{-i\kappa s}\,d\kappa$$

The function $E(\kappa)$ is called the power density spectrum $E(\kappa)$ and it represents the contribution of each range of frequencies $[\kappa, \kappa + d\kappa]$ to the energy of the signal $u'(t)$

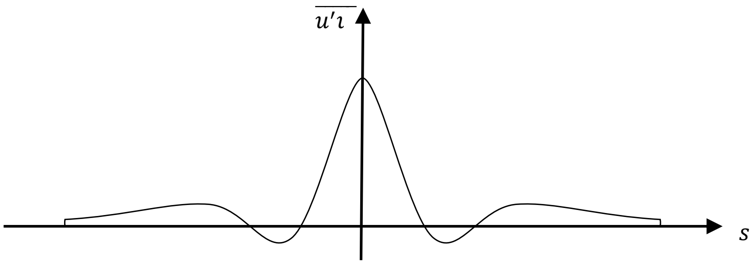

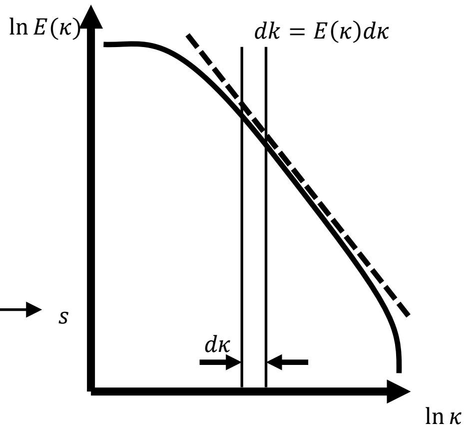

We will see later that the most important result in turbulence theory concerns the shape of energy spectra and it is still one of the very few closed-form results the study of turbulence has reached in over a century.

2.6 Checklist on correlations

- Correlations of the type

$$\sigma(\delta) = \overline{v'(t,x)v'(t,x+\delta)}$$
$$\sigma(\tau) = \overline{v'(t,x)v'(t+\tau,x)}$$

  contain information about the length- and time-scales of the turbulent flow

- The length and time-scales of turbulence
- Integral scales
- Taylor microscale
- Energy spectra: contribution of wavelength/frequency ranges to turbulence

2.7 Activity

- Modify the inputs to the matlab functions example1.m and example3.m to obtain correlation graphs of different shape. Plots can be generated with plot1.m and plot33.m (See "Correlations" folder in Canvas).
- What happens if the tensor
$$\begin{bmatrix} \alpha & \beta \\ \beta & \gamma \end{bmatrix}$$
in section 2.1.2 is not isotropic? Use the function example3.m with suitable inputs to test.
- How would you modify the functions example1.m, example2.m and example3.m to obtain the correlations directly from the input data? Could you use the results in 2.5?